PHILOSOPHICAL TRANSACTIONS OF THE ROYAL SOCIETY A MATHEMATICAL, PHYSICAL & ENGINEERING SCIENCES

Laser Radar Observations of Middle-Atmosphere Structure and Composition

L. Thomas

Phil. Trans. R. Soc. Lond. A 1987 **323**, 597-609
doi: 10.1098/rsta.1987.0108

Phil. Trans. R. Soc. Lond. A **323**, 597–609 (1987)
Printed in Great Britain

Laser radar observations of middle-atmosphere structure and composition

By L. Thomas

Department of Physics, University College of Wales, Aberystwyth, Dyfed SY23 3BZ, U.K.

A review is given of laser radar measurements of the atmosphere between about 5 and 100 km based on Rayleigh, Mie, Raman and resonance scattering processes, fluorescence and selective absorption. The results obtained with systems employing ultraviolet and visible wavelengths are examined in relation to the density and temperature structure at stratospheric and mesospheric heights, the changes in the stratospheric aerosol layer following the El Chichon eruption, the characteristics of particles in polar stratospheric clouds and of ice crystals in high-altitude cirrus clouds, and the height distributions of particular constituents. The use of infrared systems with coherent detection has, to date, been restricted to observations of Mie scattering from aerosols at heights up to the lower stratosphere. It seems likely that future developments will bring greater use of near- and middle-infrared wavelengths and probably space-borne laser radar systems.

1. Introduction

Optical probing of the atmosphere was initiated with the use of searchlights for observations of elastic backscattering. However, the type of observations possible with the technique was greatly expanded by the special features provided by lasers as sources. Specifically, the development of Q-switching provided short light pulses of large power for range-resolved measurements, and the monochromacity and beam collimation allowed discrimination against background light. The first applications of lasers to atmospheric measurements were by Fiocco & Smullin (1963) and Ligda (1963). The observations by the former workers of scattering from heights above 30 km provided an early indication of the possible use of laser probing in middle atmosphere studies. Subsequently, the technique, described by the acronym 'lidar' (light detection and ranging), has been developed for a wide range of ground-based experiments, has been employed on aircraft-borne platforms, and is being considered for space-borne operation.

The purpose of the present paper is to describe the contribution of lidar experiments to observations of structure and composition of the middle atmosphere. The principle of the technique and the optical interactions involved are described in §2. Observations of density and temperature, of stratospheric aerosols and ice crystals in clouds, and of composition are reviewed in §§3, 4 and 5, respectively. To date, little information has been derived from infrared wavelengths, except for aerosols up to lower stratospheric heights (Post *et al.* 1982; Post 1986). Consequently, attention is confined to results obtained from ultraviolet and visible wavelengths, but in outlining possible future developments in §6, mention is made of the likely increased importance of near- and middle-infrared wavelengths.

2. Remote sensing by lidar

(a) *Outline of technique*

The lidar technique involves the emission of a pulse of radiation from an appropriate laser and the measurement as a function of time, and therefore range, of the radiation backscattered by atmospheric gases and particles. The radiation collected by the receiver is passed through some form of spectrum analyser to select radiation of the required wavelength and to discriminate against background radiation. For the ultraviolet to near-infrared spectral range, photomultipliers are preferred as detectors. The output from the photomultiplier, after processing by either digital or analogue techniques, is finally passed to an appropriate recording system. Details of various lidar equipments have been reviewed by Hinkley (1976) and Measures (1984).

For a vertically directed system, in which there is a complete overlap of the transmitter and receiver fields of view, the number of photoelectrons $n_s(\lambda, h)$ generated by a pulse of radiation backscattered from a height interval Δh at a height h is given for a single scattering species, which imposes no change of wavelength, by

$$n_s(\lambda, h) = P_L(\lambda)\, T^2(\lambda, h) \frac{A}{h^2} N_i(h) \frac{d\sigma_i(\lambda)}{d\Omega} \eta \Delta h, \tag{1}$$

where $P_L(\lambda)$ represents the number of photons in the emitted laser pulse, $T(\lambda, h)$ the one-way transmission factor to height h, A/h^2 the acceptance angle of the receiver, A being the area of the mirror or lens, $N_i(h)$ the number density of the scattering species, $d\sigma_i(\lambda)/d\Omega$ the differential backscattering cross section of this species, and η the optical efficiency of the receiver system, including the quantum efficiency of the photomultiplier.

(b) *Relevant optical interactions*

Figure 1*a* represents the types of interactions used, to date, in lidar investigations of the middle atmosphere with the range of cross sections relevant to each. The corresponding constituents and parameters observed at different heights are indicated in figure 1*b*. A distinction is drawn between elastic and inelastic scattering processes.

Rayleigh scattering from molecules occurs when the frequency of the radiation does not correspond to a specific electronic transition. The differential backscatter cross section for the mixture of gases appropriate to the middle atmosphere is represented by

$$\frac{d\sigma(\lambda)}{d\Omega} = 5.45 \left[\frac{550}{\lambda(\mathrm{nm})}\right]^{4.09} \times 10^{-32}\ \mathrm{m^2\ sr^{-1}}, \tag{2}$$

where the exponent for the wavelength dependence takes account of the small correction for atmospheric dispersion (Elterman 1968). This form of elastic backscatter was observed from heights up to the middle mesosphere in the earliest lidar experiments, as reviewed by Kent & Wright (1970). Because of the wavelength dependence of cross section, Rayleigh scatter is effective only for wavelengths shorter than about 3 μm.

The second form of elastic process is that of resonance scattering from atomic or molecular species. The coincidence of the laser frequency with a specific transition of the species results in a large enhancement of cross section and ensures a good sensitivity, provided collisional quenching by other constituents is not serious. The tuning facility provided by dye lasers has

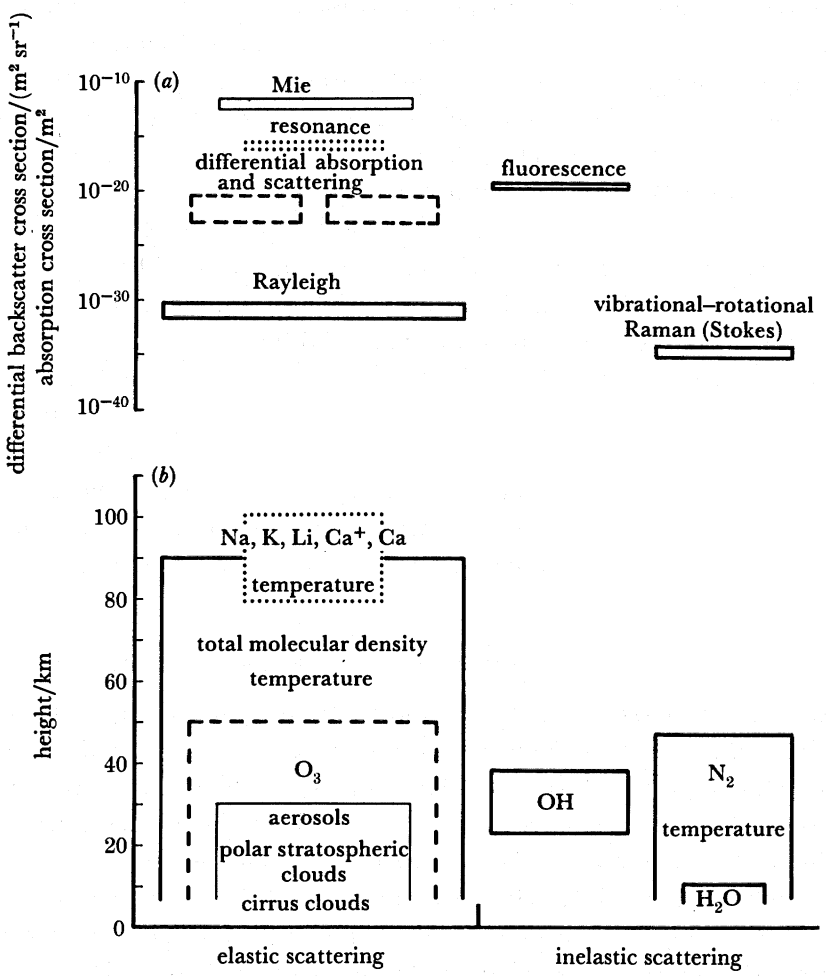

FIGURE 1. Optical interactions exploited in middle atmosphere lidar investigations (*a*), and the constituents and parameters observed (*b*). The cross sections shown in (*a*) correspond to the measurements represented by the same type of box directly below in (*b*). These latter boxes indicate the height ranges over which individual constituents or parameters have been measured.

made it possible to observe resonance scattering from neutral and ionized metal species at heights of 80–100 km, the differential cross sections being near 10^{-16} m^2 sr^{-1}. Fluorescence, shown in the inelastic category in figure 1*a*, also requires a tunable laser. Although large cross sections are again expected, the effective values are often reduced substantially by collisional quenching.

Mie scattering from stratospheric aerosols and ice crystals in clouds forms the third case of elastic scattering represented in figure 1. The sizes of these particles vary widely but the relatively large values of cross section shown in figure 1*a* accounts for the prominence of Mie scattering from the stratospheric aerosol layer in early lidar experiments (Fiocco & Grams 1964).

The second inelastic scattering process shown in figure 1*a* is vibrational–rotational Raman scattering in which the radiation undergoes a frequency change characteristic of the stationary states of the scattering molecule. The Stokes components represented in the diagram correspond to losses of energy by the radiation to molecules; the corresponding anti-Stokes components at

the shorter wavelengths have not been observed for constituents in the middle atmosphere. The characteristic Raman frequency shifts serve to identify particular molecules regardless of the irradiating wavelength although, as with Rayleigh scattering, the cross sections are proportional to the inverse fourth power of wavelength. The use of this form of scattering suffers from the relatively small cross sections. Thus the Q-branch of the nitrogen molecule, corresponding to the $\Delta v = 1$, $\Delta J = 0$ transition, has a differential Raman backscatter cross section of 4.7×10^{-35} m^2 sr^{-1} at 532 nm, compared with 6.2×10^{-32} m^2 sr^{-1} for Rayleigh scattering.

The remaining optical interaction represented in figure 1*a*, that of differential absorption and scattering, can provide greater sensitivity in measuring an atmospheric constituent than either Raman scattering or fluorescence when this is affected by quenching. In this approach, a comparison is made between the absorption of radiation tuned to correspond to an absorption line of the constituent of interest and that tuned to the wing of the line, both radiations being returned by Rayleigh, and perhaps Mie, scattering, which provides spatial resolution. The measurement is then concerned with the quantity $T(\lambda, h)$ in the radar equation (1), in contrast to the scattering measurements outlined above, which relate to the product $N_i(h)$ $[\mathrm{d}\sigma_i(\lambda)/\mathrm{d}\Omega]$. Measurements at infrared wavelengths longer than 3 μm depend on Mie scattering.

3. Measurements of atmospheric density and temperature

For heights where aerosols make no significant contribution to the elastically backscattered signal, the Rayleigh return can be used to derive the relative total molecular density as a function of height. This approach was first used with Q-switched Ruby lasers as sources (Sandford 1967) but recent studies have taken advantage of the higher pulse repetition frequencies available with Neodymium–YAG lasers, the frequency-doubled output at 532 nm being customarily employed (Chanin & Hauchecorne 1981). Still more recently, it has been claimed by Shibata *et al.* (1986) that the increased mean power of XeF excimer lasers operating at 351 and 353 nm, the increased Rayleigh scattering cross sections and larger quantum efficiencies of photomultipliers at these wavelengths all improve the technique further. It is evident that the accuracy achieved is dependent on the number of laser firings employed in the measurement, the height resolution required and the height of measurement. The measurements of Shibata *et al.* (1986), based on almost half a million firings with a 200 mJ laser in a 95 min period, provided an accuracy better than 5 % for a height resolution of 1.5 km between 30 and 70 km. Reductions in the laser beam divergence of 1 mrad and the receiver field of view of 2 mrad by an order of magnitude resulted in the upper height limit being increased to 80 km.

The assumption that the atmospheric returns are solely caused by Rayleigh backscattering by molecules generally limits the application of this approach to heights above about 30 km. The vibrational–rotational Raman returns from nitrogen are free from backscattering by aerosols, and density measurements by this approach offer a downward extension in height provided allowance is made for attenuation by aerosol and Rayleigh scatter and absorption by particular constituents, both at the incident wavelength and that of the Raman return. Garvey & Kent (1974) used a Ruby laser operating at 694.3 nm to observe the nitrogen Raman return at 828.4 nm to obtain densities with a height of resolution of 2 and 4 km between 16 and 45 km. With the improved performance offered by Neodymium–YAG and XeF excimer lasers, the advantages of operating at the shorter wavelengths provided by these sources, and the

PHILOSOPHICAL TRANSACTIONS OF THE ROYAL SOCIETY A MATHEMATICAL, PHYSICAL & ENGINEERING SCIENCES

availability of improved blocking filters for rejecting the elastically backscattered return, renewed interest is currently being shown in this approach to density measurements.

Based on the assumption of hydrostatic equilibrium and the perfect-gas law, the height variation of temperature can be deduced from the profile of relative density $N(h)$ as

$$T(h) = \frac{1}{N(h)}\left[N(h_\mathrm{m})\ T(h_\mathrm{m}) + \int_h^{h_\mathrm{m}} N(h)\, g(h)\, \mathrm{d}h\right], \tag{3}$$

where h_m represents the maximum height for which density is measured.

The analysis procedure is then to adopt a value for $T(h_\mathrm{m})$ and to calculate $T(h)$ step by step downwards, the value of $T(h_\mathrm{m})$ having little influence on the results for heights more than about 6 km below h_m. As with the density measurements, the accuracy achievable is dependent on the height resolution and the observation time. However, it seems that with the performance currently available with both Neodymium–YAG and XeF lasers, an accuracy of ± 5 K at 60 km is to be expected for measurements over about an hour with a height resolution of 1 km.

Some results derived from Rayleigh backscatter measurements carried out at Aberystwyth (52° N, 4° W) by Jenkins *et al.* (1987) are shown in figure 2. In each case the temperatures given by the CIRA (1972) model interpolated to the appropriate date and latitude are shown by the broken line. The profile for 5 June 1983 is typical of summer conditions and shows a smooth variation with height and a marked similarity to the model. By contrast, temperatures obtained in winter, even during periods that showed no stratospheric warming, as with the results for 7 November 1983, show greater variability with height and marked disagreement with the model. The profile for 1 January 1985, during a major stratospheric warming, indicates a stratopause temperature in excess of 290 K and a pronounced temperature gradient below the stratopause, amounting to 16 K km^{-1} between 34 and 36 km.

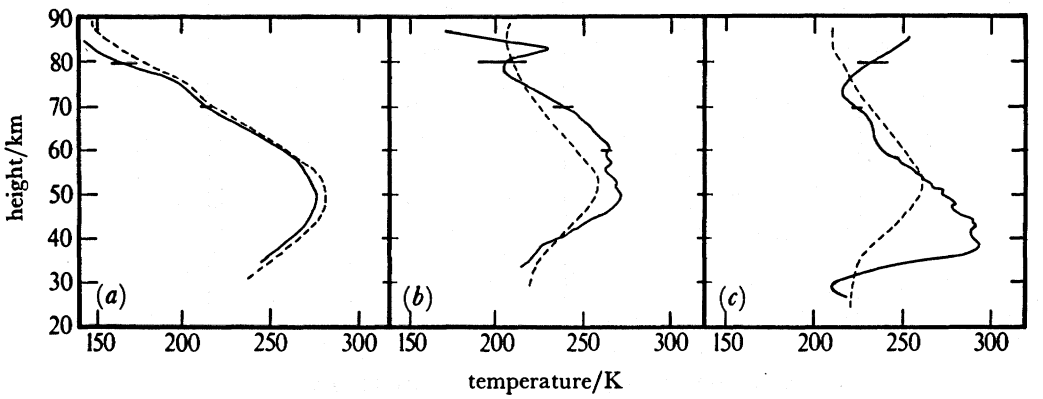

FIGURE 2. Height profiles of temperature derived from Rayleigh backscatter measurements at Aberystwyth (52° N, 4° W) and representative of (*a*) summer, 5 June 1983, and (*b*) winter, 7 November 1983, nights. Also shown is the profile observed during a major stratospheric warming (*c*), 1 January 1985. Each profile is based on about two hours of observations and shows the standard errors in derived temperatures at selected heights (Jenkins *et al.* 1987). The broken lines represent temperatures from appropriate CIRA (1972) model.

The temperature data derived from measurements of Rayleigh backscatter have been obtained up to about 80 km. For still-greater heights, between 80 and 100 km, use has been made of dye lasers to exploit the Doppler width of radiation resonantly scattered from sodium atoms (§5). Each of the sodium doublet lines is made up of two groups of hyperfine components,

each group containing two components in the case of D_1, and three in the case of D_2. In combination the lines in each group have a Doppler width at 200 K of about 1.2 pm and the two groups are separated by approximately 2 pm. Blamont *et al.* (1972) devised a method of temperature measurement in which a flashlamp-pumped dye laser was used to excite all the hyperfine components of the D_2 line and the backscattered radiation was partially absorbed in a cell containing sodium vapour at a known temperature. The reduction of the radiation in transversing the cell was a function only of the optical thickness of the sodium vapour and of the ratio of the temperature of the scattering layer to that of the cell. The disadvantage of this approach is the rather large sampling period required. In a new approach introduced by Gibson *et al.* (1979), and first used by Thomas & Bhattacharyya (1980), a laser with a linewidth of about 0.1 pm, about one thirtieth of the Doppler widths of the D_1 or D_2 complexes at temperatures in the 80–100 km height range, was used to observe the profile of the D_2 line. Because the relative strengths and frequencies of the hyperfine components are known, the line profile for any temperature can be computed. The temperature giving the best fit to the observed profile can then be established. Fricke & von Zahn (1985) have applied this method with a Neodymium–YAG pumped-dye laser providing a 0.13 pm spectral width. Their measurement of the ratio of the maximum to minimum intensity within the D_2 profile requires a relative accuracy better than 4.5% to provide an accuracy in temperature of ± 5 K at 200 K. The results obtained with 3000 laser firings occupying 200 s on the evening of 18 January 1986 at Andoya (69° N, 16° E) are shown in figure 3 (U. von Zahn, personal communication 1986). Also shown is the corresponding height variation of sodium concentration deduced from the total cross section derived from the contributions of the six hyperfine components.

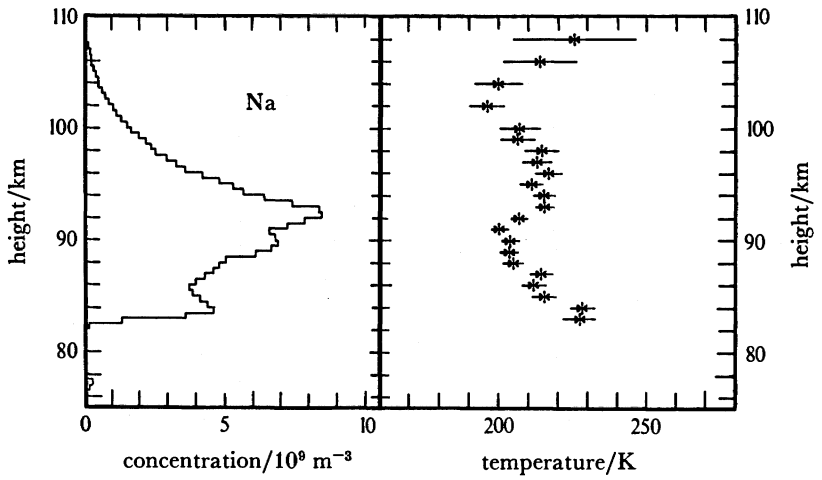

FIGURE 3. Height profiles of sodium-atom concentration and of temperature derived from measurements of resonance scattering of the sodium D_2 line at Andoya (69° N, 16° E) during 19h35–19h39 GMT on 18 January 1986 (U. von Zahn, personal communication 1986).

4. Observations of stratospheric aerosols, polar stratospheric and cirrus clouds

The use of the lidar technique at a number of sites has provided a convenient record of the stratospheric aerosol layer, monitoring the enhancement of this layer following a number of volcanic eruptions (Grams & Fiocco 1967; Russell & Hake 1977; McCormick 1982; Thomas

et al. 1983), and determining the vertical and latitudinal structure of the background layer.

The radar equation (1) for elastic scattering, can be written in the simplified form

$$n_s(h) = \frac{C[\beta_m(h) + \beta_a(h)]}{h^2} T^2(h), \tag{4}$$

where $\beta_m(h)$ and $\beta_a(h)$ represent, respectively, the molecular and aerosol differential volume backscatter coefficients and C the lidar system calibration constant. A knowledge of $\beta_m(h)$, derived from radiosonde data or an appropriate model, then provides a measure of $\beta_a(h)$ in terms of the lidar backscatter ratio

$$R = \frac{\beta_m(h) + \beta_a(h)}{\beta_m(h)}. \tag{5}$$

Height profiles of R shown in figure 4 illustrate the increase in the stratospheric aerosol layer observed at Aberystwyth following the El Chichon volcanic eruption in late March and early April 1982, and subsequent decay (Thomas *et al.* 1987); the observing system was based on a Neodymium–YAG laser operating at 532 nm. The measurement on 7 February 1983 is representative of the period of maximum backscatter from the aerosol layer, and by 31 December 1984 the layer was almost indistinguishable.

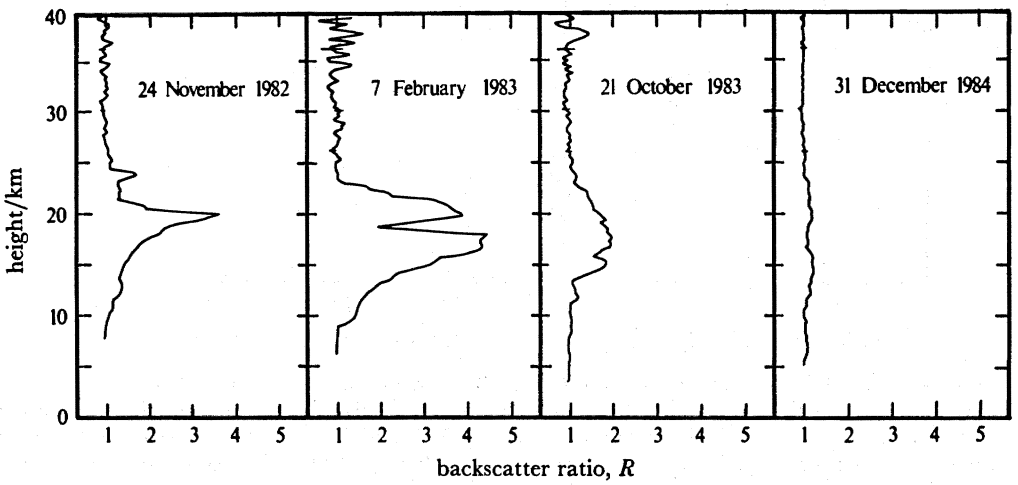

FIGURE 4. Height profiles of lidar backscatter ratio derived from measurements at Aberystwyth (52° N, 4° W) illustrating the changes in the stratospheric aerosol layer between November 1982 and December 1984. The profile for each night is based on about half an hour of observations and shows the standard errors at selected heights (Thomas *et al.* 1987).

The integrated backscatter gives an indication of aerosol loading and measurements of backscatter with good height resolution permit the study of small features as monitors of dynamical influences. Reference to figure 4 shows a pronounced minimum in the aerosol layer at about 18 km on 7 February 1983, and the height resolution of 30 m employed revealed that the backscatter ratio decreased from 4.5 to 1.5 within a height of 100 m. The change in altitude of this feature through the night was consistent with it being associated with a slowly descending isentropic surface as revealed by radiosonde data. The feature then served as a monitor of dynamical influences on that surface (Vaughan *et al.* 1987).

Observations of solar radiation at 1 μm near sunrise and sunset by the stratospheric aerosol measurement (SAM II) sensor on the *Nimbus* 7 satellite have shown enhanced aerosol extinction in the Arctic and Antarctic in winter whenever the ambient temperature falls below about 195 K (McCormick *et al.* 1982). A lidar system on board a NASA research aircraft has provided important complementary data on flights from Greenland into the polar cap (Kent *et al.* 1986). The backscatter ratio profile in figure 5*a* represents the mean of measurements over the latitude range 67.2–70.4° N, in the late afternoon of 23 January 1984, for which the mean 50 mbar† temperature was 197.5 K. This profile shows a maximum ratio of about 3 at an altitude near 14 km, with values decreasing rapidly above this height to a value of unity near 23 km indicating scattering from molecules only. The profiles in figure 5*b* show the enhancements of the backscatter at different heights, relative to that on 23 January, from measurements in the early evening of 24 January over the latitude ranges 77.2–81.5° N and 86.9–89.9° N, represented by broken and continuous lines, respectively. It is seen that enhancements by factors

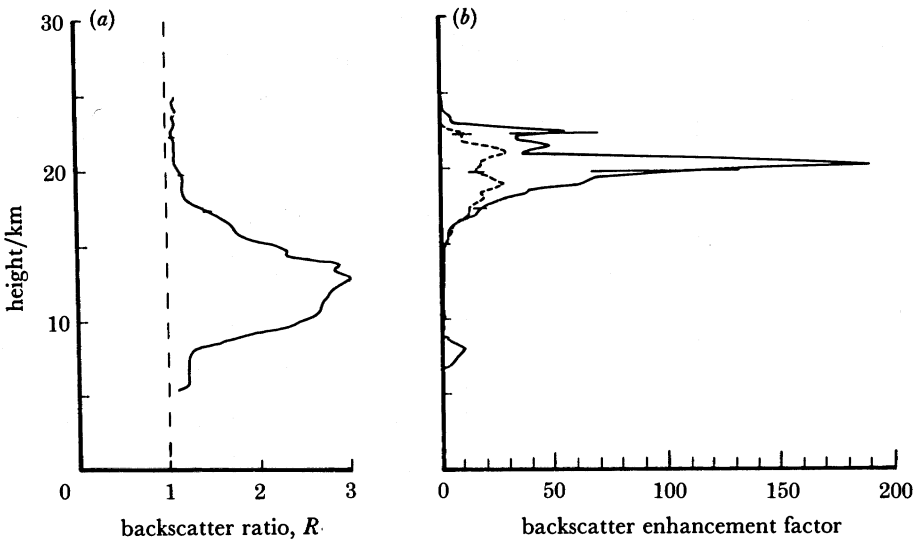

FIGURE 5. Aircraft-borne lidar measurements from Greenland showing (*a*) the profile of backscatter ratio for the latitude range 67.2–70.4° N in the late afternoon of 23 January 1984, and (*b*) the profiles of enhancement of backscatter, relative to (*a*), for the latitude ranges 77.2–81.5° N and 86.9–89.9° N, represented by broken and continuous lines, respectively, in the early evening of 24 January 1984. The standard deviations due to geographical variations are shown at selected heights (Kent *et al.* 1986).

of up to 100 were observed, the maxima occurring not at the level of maximum background aerosol, as shown in the backscatter ratio profile of 23 January, but near 20 km. The 50 mbar temperatures for these two latitude ranges on 24 January were 190.5 K and 188.0 K, respectively, and it is evident that the enhancements in backscatter increased as the lower temperatures near the Pole were approached. Measurements of the depolarization ratio of the backscattered signal revealed values between 20 and 50% for backscatter enhancements greater than 10. The implied presence of irregular ice crystals is in agreement with the theory that the polar stratospheric clouds result from a drop in stratospheric temperature causing sulphuric acid–water aerosols to be diluted by condensation of water vapour until they freeze (Steele *et al.* 1983; Kent *et al.* 1986).

† 1 mbar = 10^2 Pa.

PHILOSOPHICAL TRANSACTIONS OF THE ROYAL SOCIETY A MATHEMATICAL, PHYSICAL & ENGINEERING SCIENCES

Lidar observations of ice crystals have also been carried out at lower middle atmosphere heights, in cirrus clouds near the tropopause. An interesting feature of such lidar observations has been the evidence of a preferred horizontal orientation of plate crystals from both measurements of backscatter at different elevation angles (Gibson *et al.* 1977) and of depolarisation (Platt *et al.* 1978).

5. Observations of composition

Lidar measurements of middle-atmosphere constituents followed the development of powerful flashlamp-pumped dye lasers that could be tuned to characteristic spectral features of these constituents. Bowman *et al.* (1969) made use of such a laser to observe resonance scattering of the sodium $D_2(^2S_{\frac{1}{2}}-{}^2P_{\frac{3}{2}})$ line at 589.0 nm and, thereby, carried out the first lidar measurement of the sodium-atom concentration at mesospheric heights. Subsequent observations of the sodium layer with this technique, illustrated in figure 3, have demonstrated its diurnal and seasonal variations (Kirchoff & Clemesha 1983; Gibson & Sandford 1971), its enhancements associated with meteoric activity (Hake *et al.* 1972), and its changes under the influence of tides and gravity waves (Rowlett & Gardner 1978).

The difficulties in deriving absolute concentrations directly from the radar equation have been obviated by normalizing the backscatter from sodium atoms to the Rayleigh backscatter from a height free of aerosols, normally chosen to be above 30 km. The derivation then requires knowledge of the molecular concentration, either from an atmospheric model or from balloon-borne measurements, and of the sodium resonance and Rayleigh backscatter cross sections, together with the assumption that the atmospheric transmission up to the sodium layer is similar to that up to the normalizing height. With values of the differential backscatter cross sections of about 10^{-16} m^2 sr^{-1} for sodium atoms at mesospheric temperatures and of 4.1×10^{-32} m^2 sr^{-1} for Rayleigh backscatter, signals of the same order of magnitude are received from the two altitude regions. With systems currently used for sodium measurements, it is found that observations extending over tens of minutes provide absolute accuracies better than 30%.

The difficulty of generating radiation at 769.9 nm for resonance scattering from potassium, $K(^2S_{\frac{1}{2}}-{}^2P_{\frac{1}{2}})$, led to the replacement of flashlamps by Ruby lasers as pumps for dye lasers (Felix *et al.* 1973). Subsequent measurements of this constituent by Megie *et al.* (1978) showed no pronounced seasonal variation, in contrast to the marked enhancement in content during winter months found for sodium (Gibson & Sandford 1971; Megie & Blamont 1977) and a similar but smaller variation observed for lithium at 670.8 nm by Jegou *et al.* (1980).

The procedure of using laser-pumped dye systems was developed further by Granier *et al.* (1984) who used the harmonics of a Neodymium–YAG laser with selected dyes to produce radiations at 423 and 393 nm for observing resonance scattering from neutral and ionized calcium, respectively. The lidar observations revealed similar concentrations for these neutral and ionized atoms at mesospheric and lower thermospheric heights. This is in marked contrast to sodium for which a comparison of lidar measurements of atoms and rocket-borne mass-spectrometer measurements of ions shows an excess of the neutral form by about two orders of magnitude.

As mentioned in §2*b*, the use of fluorescence for studies of molecular constituents is restricted by collisional quenching, even at stratospheric heights. The only measurement by this approach in the middle atmosphere has been of the OH radical from a balloon (Heaps & McGee 1983,

PHILOSOPHICAL TRANSACTIONS OF THE ROYAL SOCIETY A MATHEMATICAL, PHYSICAL & ENGINEERING SCIENCES

1985). Radiation at 282 nm from a frequency-doubled dye laser, pumped by the second harmonic output of a Neodymium–YAG laser, was used to excite OH($X^2\Pi$) to the $v' = 1$ level of the $A^2\Sigma^4$ state with the aim of observing the (1, 1) transition between 306 and 315 nm. The total fluorescence efficiency calculated for the balloon flight in October 1983 (Heaps & McGee 1985), after taking account of collisional population of the $v' = 0$ level revealed by (0, 0) fluorescence, varied from 0.15 at 32 km to 0.30 at 39 km. The results of OH measurements during that flight and two subsequent flights (W. S. Heaps, personal communication 1986) show OH concentrations increasing from about 10^{12} m^{-3} to 10^{13} m^{-3} over the height range 25–38 km. As pointed out by Heaps & McGee (1985), the measured concentrations are smaller by at least a factor of 2 than the model predictions.

Uchino *et al.* (1979) showed that the absorption imposed on the radiation at 308 nm from a XeCl excimer laser can be used to estimate the height distribution of ozone. However, the estimation of the backscattered coefficients required is complicated by the presence of aerosols. The use of two closely spaced wavelengths in the differential absorption scattering technique (Schotland 1964) can obviate this difficulty and systems operating in the Hartley–Huggins bands, between 280 and 320 nm, can be used to derive information on the height distribution of ozone. The first measurements were carried out by Gibson & Thomas (1974) with a frequency-doubled flashlamp-pumped dye laser, and the technique has been developed by Pelon & Megie (1982) and Rothe *et al.* (1983). From a detailed examination of the errors involved, Pelon and Megie have shown that the optimum separation of the two wavelengths is in the range 5–15 nm. Because the choice of the absorbed wavelength is relevant to a limited range of height, pairs of wavelengths need to be chosen, from near 285 nm for the upper tropopause to 305 nm for the upper stratosphere. Figure 6 shows lidar measurements of ozone carried out at Haute Provence (44° N, 50° E) on 1 December 1981 compared with those from a balloon-borne Brewer–Mast sonde launched on 30 November (Pelon & Megie 1984). For the lidar measurements, a dye laser pumped by the frequency-doubled output of a Neodymium–

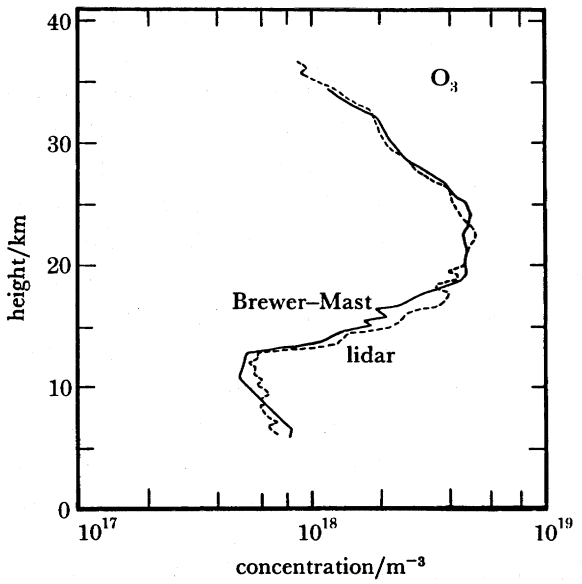

FIGURE 6. The height distributions of ozone derived from lidar measurements at Haute Provence (44° N, 50° E) on 1 December 1981 and from balloon-borne Brewer–Mast sonde measurements on 30 November 1981 (Pelon & Megie 1984).

YAG laser generated radiation between 576 and 620 nm, and frequency doubling in KDP crystals provided ultraviolet pulse energies of about 20 mJ. For the greater heights, systems taking advantage of the larger pulse energies and repetition frequencies available at 308 nm from XeCl excimer lasers are being developed. In one approach (Rothe *et al.* 1983) the second wavelength of 338 nm is generated by stimulated Raman scattering in a high-pressure methane cell; in a second approach (Pelon & Megie 1984) use is made of the third harmonic of a Neodymium–YAG laser at 355 nm as the second wavelength. However, with such large wavelength differences, errors could arise out of differences in backscatter if aerosols are present.

Reference was made in §3 to lidar observations of molecular nitrogen with vibrational–rotational Raman scattering. Such measurements, based on the frequency-tripled output of a Neodymium–YAG laser at 355 nm, at NASA Goddard (S. H. Melfi, private communication 1986) and at Aberystwyth extend to heights above 20 km. Simultaneously with the nitrogen Raman shifted wavelength, 387.5 nm, the corresponding return from water vapour, at 407.6 nm, yields relative concentration data for this constituent up to about 10 km. Comparison with *in situ* measurements then provides absolute concentrations or, alternatively, the water-vapour mixing ratio.

6. Future developments

The middle-atmosphere measurements represented in figure 1*b* have been based on the use of Ruby, Neodymium–YAG, excimer and dye lasers. With improvements in laser technology and detector sensitivity, progress can be expected in other proposed measurements in the ultraviolet to near-infrared wavelength range.

Temperature measurements based on rotational Raman scattering, fluorescence and differential absorption have been proposed, all taking advantage of the dependence of the population of molecular states on temperature through the Boltzmann term. The integrated intensity of the rotational Raman spectrum of nitrogen is relatively independent of temperature but the spectral envelope of either the O- or S-branch is a sensitive function of temperature, becoming more sharply peaked at lower values of rotational quantum number as the temperature is reduced. As first proposed by Cooney (1972), a comparison of the intensities of two regions of the spectral envelope will then provide a sensitive measure of temperature, but the major difficulty is the rejection of the elastically scattered signal. In the differential absorption approach of Kalshoven *et al.* (1981), the absorption of a laser tuned to a temperature sensitive line in the oxygen A-band near 770 nm is compared with that at an adjacent frequency having minimal resonant absorption. Developments of these two approaches are likely to be applicable to the troposphere and, therefore, contribute only to studies of the lowest part of the middle atmosphere. An approach relevant to the stratosphere has been proposed by McGee & McIlrath (1979) as an extension of the balloon-borne observations of OH fluorescence (§5). The principle is to excite two selected ground-state rotational levels and observe the fluoresence into a common vibrational band. The intensities of fluorescence should then be proportional to the initial lower-level populations and, therefore, give a measure of temperature. McGee & McIlrath estimate that a 10% accuracy in the intensity ratio corresponds to a 10 K accuracy in temperature.

Improvements in lasers and detecting systems could also provide an extension in height of constituent measurements presently confined to tropospheric heights and also initiate measurements of other constituents. Thus current water-vapour measurements from the differential

PHILOSOPHICAL TRANSACTIONS OF THE ROYAL SOCIETY A MATHEMATICAL, PHYSICAL & ENGINEERING SCIENCES

absorption and scattering approach are based on the use of two wavelengths near 720 nm (Browell *et al.* 1979). For these wavelengths, Alexandrite lasers offer certain advantages over dye lasers as sources. Greater sensitivity would be provided by the use of stronger absorption lines in the 930–960 nm range. Because of the inefficiencies of dyes in generating light at these wavelengths, the use of stimulated Raman scattering of radiation at shorter wavelengths is attractive; thus 940 nm radiation would be generated as the first Stokes line for radiation of 676 nm scattered in a high-pressure hydrogen cell (Grossmann *et al.* 1986). The location of a lidar system on an aircraft or balloon, above the highly absorbing water vapour in the lower troposphere, would be necessary to extend the measurements up to the lower stratosphere.

An extension of the wavelength of lidar systems further into the infrared region is suggested by the wealth of vibrational–rotational lines of molecules. Such an extension is also favoured by the relatively high efficiency of infrared lasers and the improved signal:noise offered by coherent detection over incoherent detection. Attention has, however, been drawn in §2*b* to the dependence on Mie scattering by aerosols for wavelengths greater than 3 μm, and the upper height limit probed with a wavelength of 10.6 μm is currently about 20 km (Post 1986). The recent development of a Neodymium–YAG coherent lidar could ensure a greater height coverage. The most immediate application of coherent lidar systems is in the measurement of winds for heights extending into the lower stratosphere, depending on the aerosol backscatter. This capability has led to an examination of the feasibility of measuring the global wind field by using a satellite-borne coherent system (Huffaker *et al.* 1984). The use of space-borne lidar systems operating over a wide range of wavelengths, to provide both synoptic coverage and good spatial resolution, is the subject of considerable study by both the European Space Agency and the U.S. National Aeronautics Space Administration. Although data relevant to weather forecasting form a major part of the initial plans, middle atmosphere studies are also represented.

References

Blamont, J. E., Chanin, M. L. & Megie, G. 1972 *Annls Géophys.* **28**, 833–838.

Bowman, M. R., Gibson, A. J. & Sandford, M. C. W. 1969 *Nature, Lond.* **221**, 456–457.

Browell, E. V., Wilkerson, T. D. & McIlrath, T. J. 1979 *Appl. Opt.* **18**, 3474–3483.

Chanin, M. L. & Hauchecorne, A. 1981 *J. geophys. Res.* **86**, 9715–9721.

CIRA 1972 *Cospar international reference atmosphere.* Berlin: Akademie-Verlag.

Cooney, J. 1972 *J. appl. Meteor.* **11**, 108–112.

Elterman, L. 1968 *Environmental research paper* no. 285, Air Force Cambridge Research Laboratories, Bedford, Massachusetts, U.S.A.

Fiocco, G. & Grams, G. 1964 *J. atmos. Sci.* **21**, 323–324.

Fiocco, G. & Smullin, L. D. 1963 *Nature, Lond.* **199**, 1275–1276.

Fricke, K. H. & von Zahn, U. 1985 *J. atmos. terr. Phys.* **47**, 499–512.

Garvey, M. J. & Kent, G. S. 1974 *Nature, Lond.* **248**, 124–125.

Gibson, A. J. & Sandford, M. C. W. 1971 *J. atmos. terr. Phys.* **33**, 1675–1684.

Gibson, A. J. & Thomas, L. 1974 *Nature, Lond.* **256**, 561–563.

Gibson, A. J., Thomas, L. & Bhattacharyya, S. K. 1977 *J. atmos. terr. Phys.* **29**, 657–660.

Gibson, A. J., Thomas, L. & Bhattacharyya, S. K. 1979 *Nature, Lond.* **281**, 131–132.

Grams, G. & Fiocco, G. 1967 *J. geophys. Res.* **72**, 3523–3542.

Granier, C., Jegou, J. P. & Megie, G. 1984 In *Proc. 12th Int. Laser Radar Conf., Aix en Provence, France* (ed. G. Megie), pp. 229–232. Service D'Aeronomie du C.N.R.S.

Grossmann, B. E., Singh, U. N., Higdon, N. S., Cotnoir, L. J., Wilkerson, T. D. & Browell, E. V. 1986 In *Proc. 13th Int. Laser Radar Conf. Toronto, Canada*, pp. 300–304. NASA conference publication no. 2431.

Hake, R. D., Arnold, D. E., Jackson, D. W., Evans, W. E., Ficklin, B. P. & Long, R. A. 1972 *J. geophys. Res.* **77**, 6839–6843.

Heaps, W. S. & McGee, T. J. 1983 *J. geophys. Res.* **88**, 5281–5289.

PHILOSOPHICAL TRANSACTIONS OF THE ROYAL SOCIETY A MATHEMATICAL, PHYSICAL & ENGINEERING SCIENCES

Heaps, W. S. & McGee, T. J. 1985 *J. geophys. Res.* **90**, 7913–7921.
Hinkley, E. D. (ed.) 1976 *Laser monitoring of the atmosphere*, pp. 1–380. Berlin, Heidelberg, New York: Springer-Verlag.
Huffaker, R. M., Lawrence, T. R., Post, M. J., Priestly, J. T., Hall, F. F., Richter, R. A. & Keeler, R. J. 1984 *Appl. Opt.* **23**, 2523–2536.
Jegou, J. P., Chanin, M. L., Megie, G. & Blamont, J. E. 1980 *Geophys. Res. Lett.* **7**, 995–998.
Jenkins, D. B., Wareing, D. P., Thomas, L. & Vaughan, G. 1987 *J. atmos. terr. Phys.* **49**, 287–298.
Kalshoven, J. E., Korb, C. L., Schwemmer, G. K. & Dombrowski, M. 1981 *Appl. Opt.* **20**, 1967–1971.
Kent, G. S., Poole, L. R. & McCormick, M. P. 1986 *J. atmos. Sci.* **43**, 2149–2161.
Kent, G. S. & Wright, R. W. H. 1970 *J. atmos. terr. Phys.* **32**, 917–943.
Kirchoff, V. W. J. H. & Clemesha, B. R. 1983 *J. geophys. Res.* **83**, 442–450.
Ligda, M. G. H. 1963 In *Proc. 1st Conf. on Laser Technology, U.S. Navy ONR, San Diego, U.S.A.*, pp. 63–72.
McCormick, M. P. 1982 In *Proc. Symposium and Workshop on Mt. St. Helens Eruption* (ed. A. Deepak), pp. 125–130. NASA conference publication no. 2240.
McCormick, M. P., Steele, H. M., Hamill, P., Chu, W. P. & Swissler, T. J. 1982 *J. atmos. Sci.* **39**, 1387–1397.
McGee, T. J. & McIlrath, T. J. 1979 *Appl. Opt.* **18**, 1710–1714.
Measures, R. M. 1984 *Laser remote sensing*, pp. 1–510. New York: Wiley.
Megie, G., Bos, F., Blamont, J. E. & Chanin, M. L. 1978 *Planet. Space Sci.* **26**, 27–35.
Megie, G. & Blamont, J. E. 1977 *Planet. Space Sci.* **25**, 1093–1109.
Pelon, J. & Megie, G. 1982 *J. geophys. Res.* **87**, 4947–4955.
Pelon, J. & Megie, M. 1984 In *Proc. 12th Int. Laser Radar Conf. Aix en Provence, France*, pp. 247–250.
Platt, C. M. R., Abshire, N. L. & McNice, G. T. 1978 *J. appl. Meteor.* **8**, 1220–1224.
Post, M. J. 1986 *J. geophys. Res.* **91**, 5222–5228.
Post, M. J., Hall, F. F., Richter, R. A. & Lawrence, T. R. 1982 *Appl. Opt.* **21**, 2442–2446.
Rothe, K. W., Walther, H. & Werner, J. 1983 *Optical and laser remote sensing* (ed. D. K. Killinger & A. Mooradian), pp. 10–16. Berlin, Heidelberg, New York: Springer-Verlag.
Rowlett, J. R. & Gardner, C. S. 1978 *Geophys. Res. Lett.* **5**, 683–686.
Russell, P. B. & Hake, R. D. 1977 *J. atmos. Sci.* **34**, 163–177.
Sandford, M. C. W. 1967 *J. atmos. terr. Phys.* **29**, 1657–1662.
Schotland, R. M. 1964 In *Proc. of 3rd Symp. on Remote Sensing of the Environment, University of Michigan, Ann Arbor, U.S.A.*, PP. 215–224.
Shibata, T., Kobuchi, M. & Maeda, M. 1986 *Appl. Opt.* **25**, 685–688.
Steele, H. M., Hamill, P., McCormick, M. P. & Swissler, T. J. 1983 *J. atmos. Sci.* **40**, 2055–2067.
Thomas, L. & Bhattacharyya, S. K. 1980 In *Proc. 5th Rocket and Balloon Programmes and Related Research*, ESA SP-152, pp. 49–50.
Thomas, L., Jenkins, D. B., Wareing, D. P. & Farrington, M. 1983 *Nature, Lond.* **304**, 248–250.
Thomas, L., Jenkins, D. B., Wareing, D. P., Vaughan, G. & Farrington, M. 1987 *Annls Geophys.* **5A**, 47–56.
Uchino, O., Maeda, M. & Hirono, M. 1979 *J. quant. Elect.* **QE-15**, 1094–1107.
Vaughan, G., Jenkins, D. B., Thomas, L., Wareing, D. P. & Farrington, M. 1987 *Tellus.* (In the press.)

PHILOSOPHICAL TRANSACTIONS OF THE ROYAL SOCIETY A MATHEMATICAL, PHYSICAL & ENGINEERING SCIENCES